Available online at www.sciencedirect.com
SCIENCE DIRECT®
Surface Science 592 (2005) 150–158
SURFACE SCIENCE
www.elsevier.com/locate/susc

Structural transitions of chemisorbed iodine on Au(100): A STM and LEED study

J. Valenzuela-Benavides *, M. Herrera-Zaldívar

Centro de Ciencias de la Materia Condensada, Universidad Nacional Autónoma de México, Apdo. Postal 2681, Ensenada, 22800 BC, Mexico

Received 30 April 2005; accepted for publication 7 July 2005
Available online 25 July 2005

Abstract

We have studied the chemisorption of molecular iodine on a reconstructed Au(100) surface by means of low energy electron diffraction (LEED) and scanning tunneling microscopy (STM) in an ultra high vacuum environment at 300 K and at temperatures down to 115 K. Several structural phases are observed during iodine adsorption. At 300 K, a low iodine coverage of $\theta_I \sim 0.1$ ML is sufficient to lift the "hex" reconstruction, producing the substrate's (1×1) diffraction pattern with a diffuse background. The first stable structure defined as $c(p\sqrt{2} \times 2\sqrt{2})R45°$, is formed at coverages slightly higher than 0.4 ML that uniaxially compresses with increasing iodine coverage. For higher coverages $\theta_I > 0.5$ ML the iodine layer transforms to a rotated hexagonal structure with a maximum angle of 3.5° with respect to the [001] substrate direction. An iodine structure not previously reported for this system was observed to form at $T \sim 120$ K when $\theta_I \sim 0.33$ ML, and only observable under certain adsorption/cooling conditions. The findings are discussed in terms of the subtle competition between adsorbate–substrate and adsorbate–adsorbate interactions in determining the adsorbate structure.

Keywords: Iodine; Gold; Scanning tunneling microscopy; Electron diffraction; Chemisorption; Surface structure; Solid–vacuum interfaces

1. Introduction

Halogen adsorption on metal surfaces has been investigated extensively in the past using low energy electron diffraction (LEED) and surface X-ray scattering (SXS) techniques in ultrahigh vacuum (UHV) and electrolyte solution respectively, and more recently with in situ scanning

* Corresponding author. Address: CCMC-UNAM, P.O. Box 439036, San Ysidro, CA 92143-9036, USA. Tel.: +52 646 174 4602; fax: +52 646 174 4603.
E-mail address: valenzue@ccmc.unam.mx (J. Valenzuela-Benavides).

0039-6028/$ - see front matter © 2005 Elsevier B.V. All rights reserved.
doi:10.1016/j.susc.2005.07.004

tunneling microscopy (STM) [1–4]. Iodine adsorption on Au(1 0 0) has not been so extensively studied as Au(1 1 1), and only limited information can be found in the literature about structural transitions in UHV conditions. Neumann et al. [5] studied iodine adsorption on Au(1 0 0) using LEED and thermal desorption spectroscopy (TDS), where they reported the formation of an incommensurate c($p\sqrt{2}\times 2\sqrt{2}$)$R45°$ structure beginning at $\theta_I = 0.42$ ML that transforms to a so-called "compression" structure as θ_I approaches 0.5 ML, with a saturation coverage reaching a maximum value of 0.56 ML. They also reported that upon adsorption at a slightly lower temperature or by annealing the $\theta_I = 0.5$ phase the formation of a commensurate c($\sqrt{2}\times 2\sqrt{2}$)$R45°$ phase was possible. No detailed explanation of the observed diffraction patterns in terms of real-space structural models was presented by the authors.

An in situ STM study in an electrochemical environment revealed a series of potential-dependent iodine phases, beginning at $\theta_I = 0.46$ with a compressible incommensurate c($p\sqrt{2}\times 2\sqrt{2}$)$R45°$ structure which reverted to a commensurate c($\sqrt{2}\times 2\sqrt{2}$)$R45°$ at $\theta_I = 0.5$. At higher potential (increased coverage) a pseudo-hexagonal adlayer formed with a slight rotation with respect to the Au(1 0 0) substrate [6].

Here we report a variable temperature study of the adsorption of iodine on Au(1 0 0) using a combination of LEED and STM techniques that complements the above cited studies, with the hope that it will provide a better understanding of the differences and similarities between the solid/vacuum and solid/electrolyte interfaces concerning halogen adlayers on metal surfaces. We also present results of a new iodine structure stable at low temperatures and observable only under certain adsorption/cooling conditions. The results are discussed in terms of competing adsorbate–substrate and adsorbate–adsorbate interactions mediated by substrate temperature.

2. Experimental details

Experiments where carried out in an ultra high vacuum system equipped with a quick sample introduction load-lock, a reverse view LEED (VG Instruments) and a lab-built ambient temperature STM. Working pressure during iodine adsorption was kept below 1×10^{-10} mbar. A special heating/cooling sample stage was constructed for the multi-axis manipulator (VG Instruments) that permitted transfer of the sample between the different instruments with the help of a long travel wobble-stick. The sample holder was made of a molybdenum sheet that included its own thermocouple welded close to the sample, with the gold single crystal fixed to this plate using tantalum wire. Heating was achieved by direct filament radiation and electron bombardment. For cooling the sample, nitrogen gas flowed through a copper coiled tubing immersed in a Dewar filled with liquid nitrogen and then through a heat-transfer unit inside the chamber that included a heavy copper braid and plate where a second thermocouple was fixed.

For the iodine source we constructed a solid state electrochemical cell following a reliable design that uses a Ag_4RbI_5 pellet: a high ionic-conductivity compound sandwiched between two Pt electrode meshes that serve as electrodes [7]. The use of this design presents several advantages: dosing amounts are highly controllable since they are proportional to the Faraday current in the cell. Also exposure and coverage calibration is less complicated than gas admission into the chamber, and operates at room temperature. Typical cell currents in our experiments range between 25 and 100 μA, enough to complete a full iodine monolayer in less than a minute. During operation of the cell only a slight increase of background pressure was detected.

The Au(1 0 0) single crystal was supplied cut and polished by a commercial vendor (SPLabs, Holland), and no further treatment was done except for ultrasonic cleaning in acetone and annealing in UHV. For STM imaging electrochemically etched W tips were used, with typical tunneling parameters of: below 25 mV for the sample bias and currents from one up to several nA. All STM images presented here where taken in topographical/constant current mode.

3. Results and discussion

3.1. LEED results

After the introduction of the gold single crystal into the chamber, the sample was annealed at 900 K for several hours and allowed to cool to room temperature. Fig. 1 shows a sequence of LEED patterns observed before and after iodine adsorption onto a Au(100) surface at 300 K, beginning with the characteristic diffraction pattern of the clean reconstructed "hex" surface in Fig. 1(a). Exposure of this surface to the iodine beam lifted the reconstruction at $\theta_I \sim 0.15$ ML,

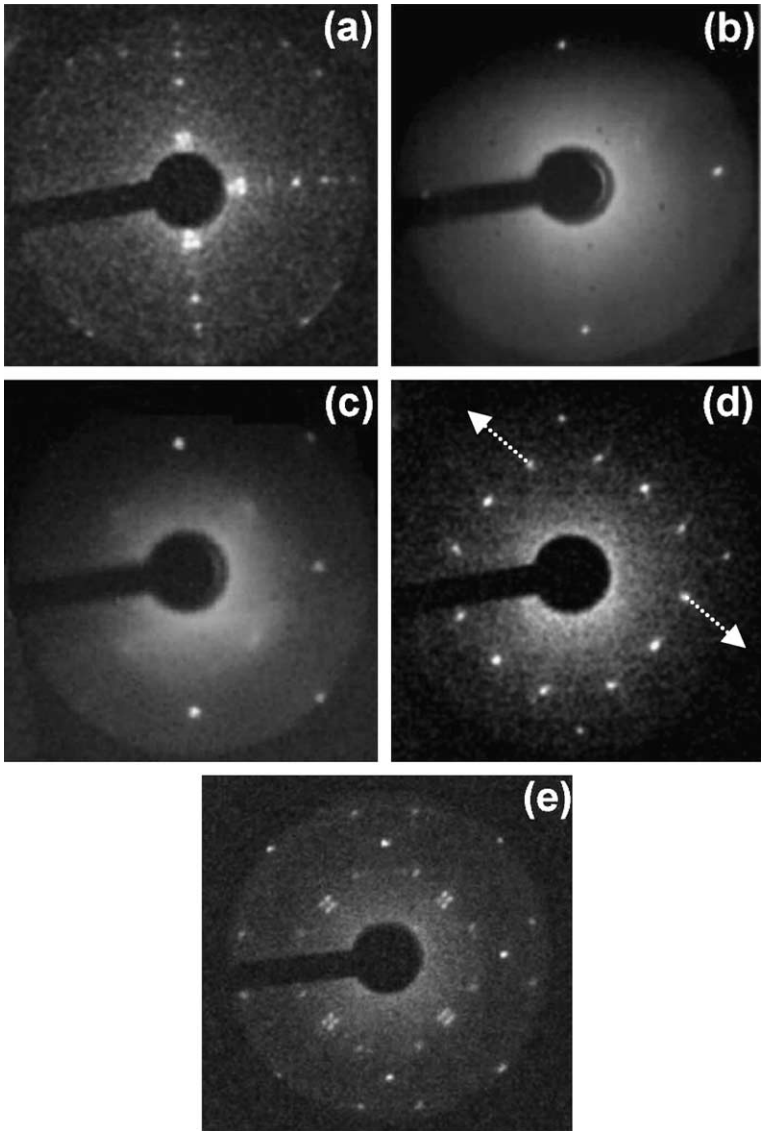

Fig. 1. Sequence of LEED diffraction patterns (a) before and (b–e) after iodine adsorption at 300 K. (a) "hex"-Au(100); (b) (1×1)-Au(100) for $\theta_I \sim 0.15$ ML; (c) $\theta_I \sim 0.3$ ML; (d) $c(p\sqrt{2} \times 2\sqrt{2})R45°$ for $\theta_I \sim 0.45$ ML; (e) "rot-hex" saturation structure at $\theta_I \sim 0.56$ ML. Beam energy: (a–d): 51 eV; (e): 61 eV.

producing the diffraction pattern corresponding to the (1×1) surface as shown in (b) with a noticeable increase in background intensity. Further exposure produced a diffuse pattern around $\theta_I \sim 0.3$ ML as shown in (c). The first diffraction pattern with well-defined spots arranged in a circular geometry around the (0 0) beam was observed at a coverage around 0.45, as shown in (d). Increased adsorption caused the displacement of two of the spots along the direction of the arrows as depicted in (d), while the half order spots remained in a fixed position. This diffraction pattern, which includes contribution from two domains due to the twofold symmetry of the substrate, corresponds to a pseudo-hexagonal supercell defined as $c(p\sqrt{2} \times 2\sqrt{2})R45°$ that continuously compresses along the $p\sqrt{2}$ direction with increasing iodine coverage, from a nearest neighbor spacing (NNS) close to 4.5 Å down to approximately 4.2 Å, and 4.6 Å along the other atomic row directions. The p parameter is used here in the same context as defined by Gao et al. in their study of iodine adsorption on Au(1 0 0) in an electrochemical environment [6] and referring to the amount of uniaxial compression, where higher values of p correspond to a more compressed structure, hence the $p\sqrt{2}$ term relates to the largest dimension (periodicity) of the supercell. Fig. 2(a) shows the unit vectors in reciprocal space for a single domain and the real-space model of the $c(p\sqrt{2} \times 2\sqrt{2})R45°$ iodine structure. The reason for choosing the particular iodine positions shown in (b) will become clear when the STM data is presented.

When coverage reaches $\theta_I \sim 0.5$ ML a structural transition occurs, characterized by a splitting of the half order spots into four spots as the diffraction pattern in Fig. 1(e) shows. These spots move away from each other until the coverage reaches saturation around $\theta_I \sim 0.56$ ML. Inspection of the LEED pattern reveals that it corresponds to a pseudo-hexagonal iodine adlayer that rotates continuously a maximum of $\pm 3.5°$ with respect to the substrate's $\sqrt{2}$ direction with increasing coverage. Gao et al. estimated this angle to be $\sim 5°$ using STM images [6], which is a less accurate method than LEED because of x–y distortions. NNS for this structure is around 4.3 Å, i.e., iodine–iodine separation has relaxed in the $\sqrt{2}$ and decreased in the other two directions between 4.3 and 4.4 Å, a decreased from its previous value of 4.6 Å. This rotated pseudo-hexagonal structure will be referred hereafter as the "rot-hex" structure.

Interestingly, we could reverse the diffraction pattern sequence shown in Fig. 1 that corresponds to room temperature adsorption by inducing a very slow desorption of iodine with the LEED

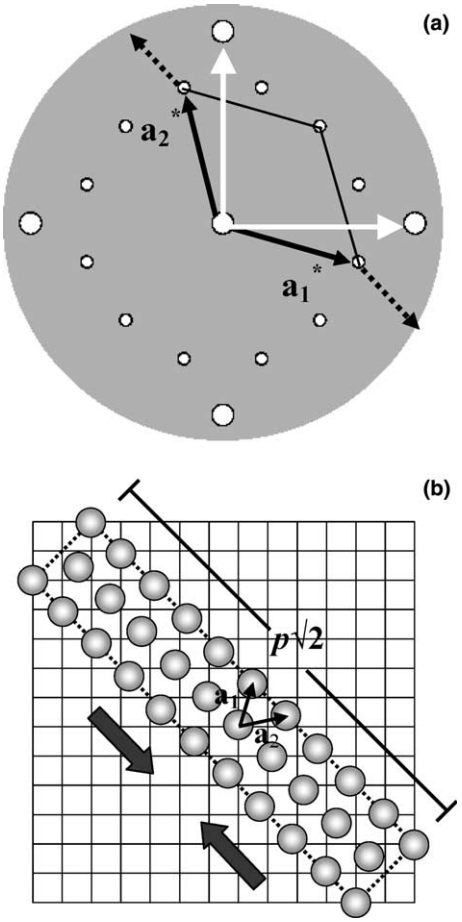

Fig. 2. (a) Diffraction pattern representation for the $c(p\sqrt{2} \times 2\sqrt{2})R45°$ structure showing the substrate's (large circles) and adlayer's (small circles) diffraction spots with their respective reciprocal lattice vectors. Dotted line arrows indicate the displacement direction of the spots during compression of the adlayer. (b) Sphere model of the iodine adlayer with respect to the square lattice, where $p = 11$ for this particular coverage. Thick arrows indicate the direction of compression.

electron beam: starting with the saturation pattern, the four split-spots shown in Fig. 1(e) collapse into a single spot in the (1/2, 1/2) position, followed by the displacement of spots shown in (d) in the reverse direction of the arrows. Even though the electron beam induced desorption is rather slow, sample exposure to the beam was limited only for short time intervals during LEED experiments.

3.2. Low temperature LEED

The above results are in excellent agreement with those reported by Neumann et al. [5] except for the LEED pattern corresponding to the semi-diffuse phase shown in Fig. 1(c), which led us to explore this particular adsorption coverage ($\theta_I \sim 0.3$) in more detail. It is expected from entropic considerations that by lowering the surface temperature long range order could be achieved as the iodine adatoms in the liquid-like adlayer reduce their mobility and adatom–substrate interactions begin to dominate over the adsorbate–adsorbate repulsive interaction, resulting in a more stable periodic structure not possible at higher temperatures. To ascertain if this was the case for the particular coverage in question, a ~0.3 coverage of iodine was deposited on a clean reconstructed Au(1 0 0) surface at 300 K, forming the diffraction pattern similar to the one shown in Fig. 1(c), followed by cooling of the sample at a rate of 12 K/min. A sequence of the resulting LEED patterns are shown in Fig. 3, where at a temperature of 126 K a definite long range structure emerges (d) that becomes better defined at 116 K (f), although some remnant disorder is still present as indicated by the elongated spots. Unfortunately we were not able to lower the temperature further, which might have eliminated the elongated spots completely. LEED pattern simulation shows that this final diffraction pattern corresponds to a $c(6\times 2)$ structure.

We discarded the possibility that an adsorbed species of a foreign nature (e.g. residual chamber gases) could be responsible for the observed $c(6\times 2)$ structure by repeating a similar low temperature experiment starting with a clean reconstructed surface (no iodine deposition). Results showed only the presence of the stable "hex" reconstruction down to 116 K as expected.

3.3. STM results

Before STM imaging, a particular iodine structure was first determined by LEED diffraction before the sample was transferred to the STM. Fig. 4(a) shows an atomic resolution image of the $c(p\sqrt{2}\times 2\sqrt{2})R45°$ structure with $\theta_I = 0.45$ corresponding to diffraction pattern in Fig. 1(d). Every atomic row has a characteristic long range periodic modulation that runs vertically in the image, alternating in intensity from bright to dark with a periodicity of approximately eleven iodine–iodine distances, making $p \approx 12$ in this image. As typical for halogen adsorption on metals, the greyscale intensity in the STM image relates simply to the topographical corrugation produced by different adsorption sites: brighter spots are associated with atoms protruding from the surface and vice versa.

In order to better understand the origin of the periodic modulations or Moiré patterns observed in the STM images we used a previously reported procedure for simulating images known as the "hard-ball contact model", where a computer generated adlayer lattice is superimposed over the substrate's lattice of the desired symmetry. It was applied successfully for simulating iodine adlayers on Au(1 1 1) and Ag(1 1 1) surfaces [8]. Fig. 4(b) shows a computer simulated image obtained for a pseudo-hexagonal lattice on top of Au(1 0 0) square lattice together with its Fourier transform (FT) (c), following the supercell orientation presented in Fig. 2(b). It can be seen that it reproduces quite well all the characteristics of the STM image and the observed LEED diffraction pattern for this structure. We can therefore conclude that the periodic modulation is a consequence of the different adsorption sites for iodine along the $\sqrt{2}$ direction: higher "on-top" positions in corner atoms of the supercell, and lower "four-fold" positions in center regions. The interatomic distances used for this particular iodine adlattice simulation were 4.4 Å in the compression direction ($\sqrt{2}$ direction) and 4.6 Å in the other two atomic

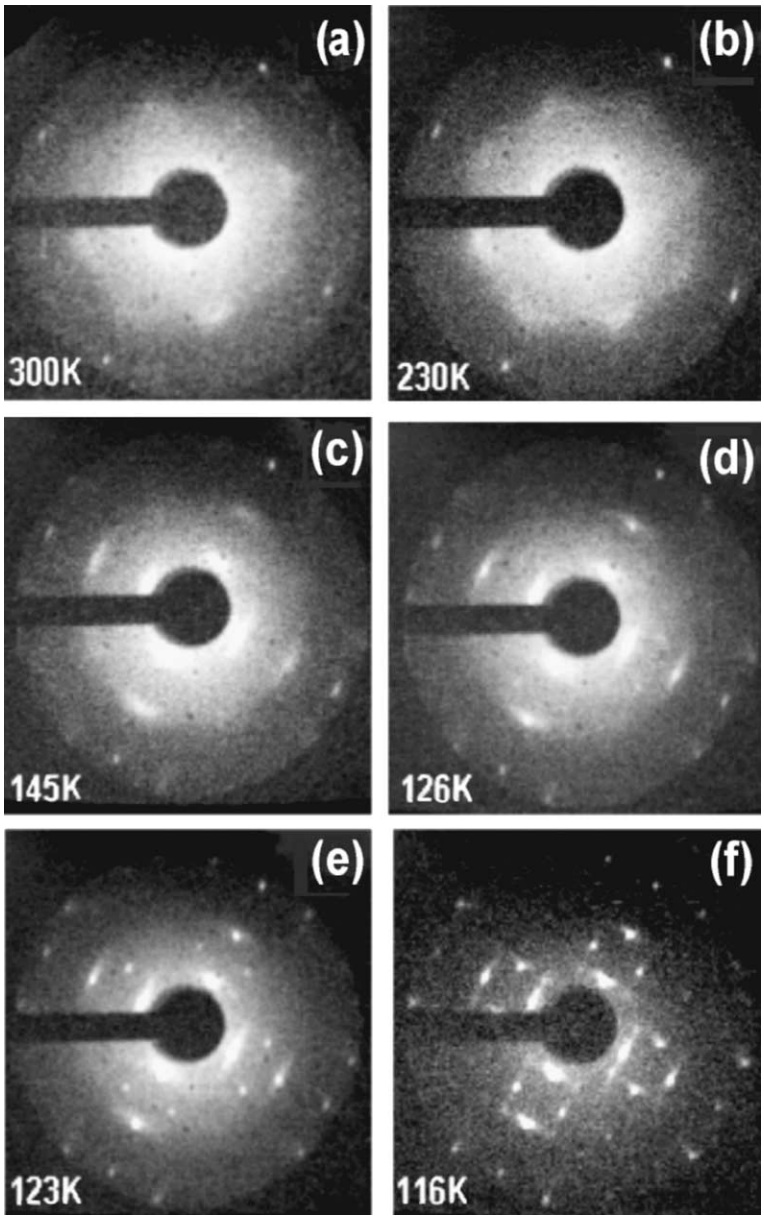

Fig. 3. Sequence of diffraction patterns for an iodine coverage of ~0.3 ML at different temperatures showing the final formation of the c(6 × 2) structure. Beam energy: 34 eV.

rows directions, which can be described as a $c(12\sqrt{2} \times 2\sqrt{2})R45°$ coincidence supercell.

The STM image corresponding to the diffraction pattern in Fig. 1(e) or ''rot-hex'' structure with iodine coverage slightly higher than 0.5 ML is shown in Fig. 5(a). Like the previous image, it also has a strong periodic modulation of bright and dark strips running diagonally from the top-left corner to bottom-right corner with a ~30 Å period at an angle of about 47° with respect to the atomic rows indicated by the arrow. Along this direction each atomic row alternates in intensity,

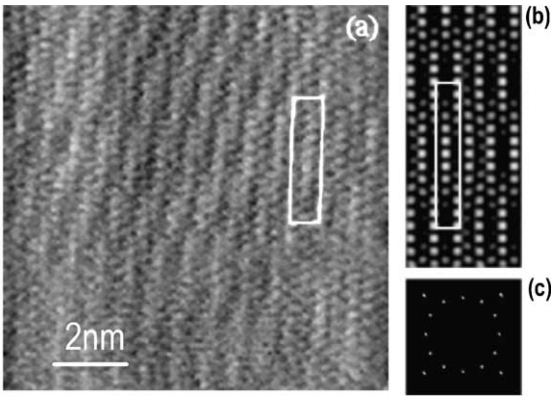

Fig. 4. (a) $10.6 \times 10.6\ \mathrm{nm}^2$ STM image of the c($p\sqrt{2} \times 2\sqrt{2}$)$R45°$ structure with $p = 12$ corresponding to a coverage $\theta_I = 0.45$ ML. Tunneling parameters: $I_T = 6$ nA, $V = +10$ mV. (b) Simulated image using the "hard-ball" contact model and its (c) FT with contributions from two domains.

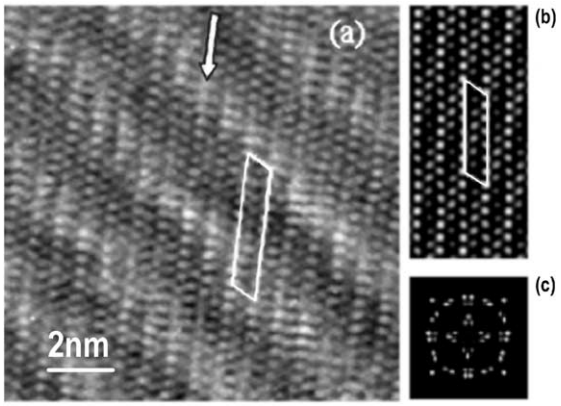

Fig. 5. (a) $12 \times 12\ \mathrm{nm}^2$ STM image of the "rot-hex" iodine structure showing the characteristic Moiré patterns. Tunneling parameters: $I_T = 2.4$ nA, $V = +10$ mV. (b) Simulated image using the "hard-ball" contact model and its (c) FT with contributions from two domains.

indicating iodine atomic positions of higher and lower height with respect to neighboring atoms, while atomic rows at either side of the arrow have a less pronounced height modulation.

The simulated image presented in (b) was generated by a 3.5° counter-clockwise rotation of a pseudo-hexagonal lattice with respect to the substrate's $\sqrt{2}$ direction. The resulting Moiré pattern reproduces all the features of the experimental image described above, and also a good resemblance is found between its FT shown in (c) with the diffraction pattern in Fig. 1(e).

As a final note regarding this section we point out that it was not possible to obtain STM images of the low temperature phase observed by LEED, since our instrument only operates at room temperature. Nevertheless, we can make a reasonable assumption that the structural model proposed by Andryushechkin et al. [9] of the c(6×2) observed at room temperature for I–Cu(100) may be applied here for I–Au(100) observed at low temperature.

4. Further discussion

As pointed out earlier, a c(6×2) structure has not been reported for iodine on Au(100), although Neumann et al. performed a similar low-temperature adsorption experiment in UHV [5]. A reasonable explanation for this discrepancy is the way the adsorption and cooling process was performed: they made an adsorption experiment at 130 K where the adatoms simply did not have the required mobility to produced long range order, as a consequence of this no well-order structure was observed up to a monolayer coverage. In our case, we adsorbed iodine then lowered the temperature, facilitating the adatoms to slowly adopt the observed c(6×2) metastable structure. Jones and Perry reported a similar temperature dependence of the structural phases of iodine on Fe(100), where the order of the adsorption/heating steps was relevant in determining the final observed structure [10].

Furthermore, theoretical studies of halide adlayers on the (100) surface of fcc metals indicate that ordering in low-density phases such as the p(2×2) or c(2×4), where $\theta \sim 1/4$ ML, are only possible at low temperatures [11,12]. The symmetry of the Au(100) surface differs from the intrinsic symmetry of the iodine adlayer, which tends to form incommensurate pseudo-hexagonal structures due to the strong adsorbate–adsorbate interaction. On the other hand, if the adsorbate–substrate interactions are dominant, the adlayer should adopt the substrate symmetry, as long as the structural mismatch is not too high [13].

Our observation of the low-density phase c(6 × 2) at $\theta_I \sim 0.3$ hence can be explained in terms of a stronger adsorbate–substrate interaction dominating over a weaker adsorbate–adsorbate interaction, promoted by a lower temperature. In these terms, it would then seem possible that a c(6 × 2) phase could form at room temperature if only the substrate's potential corrugation is made strong enough so that repulsive adsorbate–adsorbate interactions are overcome. This is indeed the case for Cu(1 0 0), where the iodine adlayer forms a c(6 × 2) at $\theta_I = 0.33$ at room temperature [9]. Even though the Cu lattice parameter is 13% smaller than that of gold, the increased repulsive interaction between iodine atoms is overcome by the higher binding energy to the Cu substrate. Calculations have shown that halide adlayers on (1 0 0) metal surfaces tend to form commensurate structures, mainly c(2 × 2), reflecting the higher substrate corrugation potential [14], even if it means overcoming the strong iodine–iodine repulsive interaction due to a smaller NNS below the van der Waals diameter (4.3 Å). Well known examples are Pt [15], Pd [16], Ag [17].

Another important point that elucidates the subtle competition between adsorbate–substrate and adsorbate–adsorbate interaction in determining the structure of an adsorbed iodine layer can be understood if we compared our results with those reported by Gao et al. for iodine adsorption on Au(1 0 0) in an electrochemical environment [6]. They reported that for a coverage below 0.5 ML, the first structure that forms is the uniaxial incommensurate c($p\sqrt{2} \times 2\sqrt{2}$)$R45°$ that transforms to the commensurate c($\sqrt{2} \times 2\sqrt{2}$)$R45°$ when $\theta_I = 0.5$, then to a slightly rotated pseudo-hexagonal structure for $\theta_I > 0.5$ until saturation occurs at $\theta_I = 0.56$. In our UHV experiments at room temperature, the incommensurate c($p\sqrt{2} \times 2\sqrt{2}$)$R45°$ structure transforms directly to the rotated pseudo-hexagonal structure at $\theta_I \sim 0.5$, and the commensurate c($\sqrt{2} \times 2\sqrt{2}$)$R45°$ appears only when the temperature of the substrate is lowered (~250 K), in agreement with results reported by Neumann et al. [5]. These experiments again suggest that, in UHV conditions, lowering the temperature of the substrate decreases adsorbate–adsorbate interaction until the adsorbate–substrate interaction dominates, "locking" iodine atoms in bridge positions to form the c($\sqrt{2} \times 2\sqrt{2}$)$R45°$ commensurate structure. These differences can be attributed to the distinct environments between the solid/vacuum and solid/electrolyte interfaces, since the dipole moments obtained for electrochemically adsorbed species are generally smaller than in UHV due to the presence solvated ions in solution in the latter case.

A final point regarding the stability of the observed iodine structures at room temperature. It is well known that near saturation coverage a rotated hexagonal iodine adlayer forms on Au(1 1 1) in electrochemical solutions under potentiostatic control [8,18] and in UHV conditions [19], with a similar iodine packing density ($\Gamma \sim 6 \times 10^{14}$ cm^{-2}) as in the Au(1 0 0) surface. In both cases the structure is unstable when: (1) the crystal is taken out the electrochemical cell, and (2) in UHV when the iodine gas pressure in the system drops below a critical threshold of ~10^{-6} mbar, reverting to a lower coverage structure [19]. This is in sharp contrast to the highly stable "rot-hex" structure on Au(1 0 0) that we could observe for days after initial adsorption in UHV and in ambient conditions [20]. The notable stability is a reflection of the higher substrate corrugation potential on the more open, square (1 0 0) lattice. To our knowledge no reports can be found in the literature on the stability of the "rot-hex" iodine structure on Au(1 0 0) after it emerges from an electrochemical cell once it has formed under potentiostatic control. Our results suggest that it would be highly stable in ambient conditions.

5. Conclusions

As demonstrated in this work and proven by a growing body of literature, LEED and STM are powerful complementary techniques for studying surface structures. Although STM lacks the spatial accuracy that other surface techniques posses for determining interatomic distances (e.g. LEED, SXS), its sensitivity to surface atomic corrugation can be used successfully to reveal valuable information on the relative position of the adlayer with respect to the substrate. In this work, a simple

"hard-ball" model has been applied that accounts for the observed surface features and Moiré patterns of the iodine adlayer on Au(100) that demonstrates identical structures as in an electrochemical environment.

Finally, a careful examination in the low temperature regime has revealed an iodine structure on Au(100) not previously reported. A discussion was presented in terms of competing adsorbate–substrate and adsorbate–absorbate interactions.

Acknowledgements

The authors express their gratitude to Dr. Leonardo Morales de la Garza for the useful discussions during the course of this work. This work was supported by Grant No. IN113303 from PAPIIT-UNAM.

References

[1] R.G. Jones, Prog. Surf. Sci. 27 (1988) 25.
[2] O.M. Magnussen, Chem. Rev. 102 (2002) 679.
[3] A.A. Gewirth, G.K. Niece, Chem. Rev. 97 (1997) 1129.
[4] M.P. Soriaga, Prog. Surf. Sci. 39 (1992) 325.
[5] A. Neumann, K. Christmann, T. Solomun, Surf. Sci. 287 (1993) 593.
[6] X. Gao, G.J. Edens, F.C. Liu, A. Hamelin, M.J. Weaver, J. Phys. Chem. 98 (1994) 8086.
[7] S.A. Furman, D.A. Harrington, J. Vac. Sci. Technol. A 14 (1996) 256.
[8] T. Yamada, N. Batina, K. Itaya, J. Phys. Chem. 99 (1995) 8817;
N. Batina, T. Yamada, K. Itaya, Langmuir 11 (1995) 4568;
T. Yamada, K. Ogaki, S. Okubo, K. Itaya, Surf. Sci. 369 (1996) 321.
[9] B.V. Andryushechkin, K.N. Eltsov, V.M. Shevlyuga, U. Bardi, B. Cortigiani, Surf. Sci. 497 (2002) 59.
[10] R.G. Jones, D.L. Perry, Surf. Sci. 88 (1979) 331.
[11] K. Binder, D.P. Landau, Surf. Sci. 61 (1976) 577.
[12] S.J. Mitchell, G. Brown, P.A. Rikvold, Surf. Sci. 471 (2001) 125.
[13] J.A. Venables, The Chemical Physics of Solid Surface, vol. 8, Elsevier, Amsterdam, 1997, p. 1.
[14] A. Ignaczak, J.A.N.F. Gomes, J. Electroanal. Chem. 420 (1997) 71.
[15] C.M. Vitus, S.-C. Chang, B.C. Schardt, M.J. Weaver, J. Phys. Chem. 95 (1991) 7559.
[16] K. Sashikata, Y. Matsui, K. Itaya, M.P. Soriaga, J. Phys. Chem. 100 (1996) 20027.
[17] T. Teshima, K. Ogaki, K. Itaya, J. Phys. Chem. B 101 (1997) 2046.
[18] B.M. Ocko, G.M. Watson, J. Wang, J. Phys. Chem. 98 (1994) 897.
[19] S.A. Cochran, H.H. Farrell, Surf. Sci. 95 (1980) 359.
[20] A. Gonzalez-Carrazco, J. Valenzuela-Benavides, unpublished results.